Kinetics of the eutectoid transformation in the Cu–In system

A. DAS, S. K. PABI, I. MANNA*
Metallurgical and Materials Engineering Department, Indian Institute of Technology, Kharagpur, W.B. 721 302, India

W. GUST
Institute für Metallkunde, University of Stuttgart, Seestr. 75, 70174 Stuttgart, Germany
E-mail: bonny@hijli.iitkgp.ernet.in

The present study concerns a detailed investigation of the kinetics of the eutectoid transformation in the Cu–In system based on both the isothermal growth rate of the eutectoid colony (monitored by microstructural change) and enthalpy changes during non-isothermal heating (determined by differential scanning calorimetry) of solution-treated and quenched samples. The maximum growth distance of the eutectoid cells and the equilibrium interlamellar spacing have been determined by optical and scanning electron microscopy in the temperature range 600–825 K. The reaction front velocity was observed to increase with the isothermal ageing temperature in the temperature range studied. A detailed analysis of the isothermal growth kinetics through the models available in the literature has yielded an activation energy of 125–127 kJ mol^{-1} for the operating diffusion process, which is comparable with that for discontinuous precipitation in Cu–In or for grain boundary tracer diffusion of ^{115}In in Cu, but significantly lower than that for volume diffusion of In in the β Cu–In alloy. A subsequent differential scanning calorimetric study has indicated a similar activation energy of 133 kJ mol^{-1} for the concerned eutectoid transformation. It is thus concluded that the eutectoid transformation in the Cu–In system is a boundary-diffusion-controlled process. © *1999 Kluwer Academic Publishers*

1. Introduction

The eutectoid transformation in a binary system may be defined as a solid-state diffusion-controlled decomposition process of a high temperature phase into a two-phase lamellar aggregate behind a migrating boundary on cooling below the eutectoid temperature (T_{eu}) [1]. In Cu–In, this transformation occurs as $\beta \rightarrow \alpha + \delta$ at 20.15 at % In below $T_{eu} = 847$ K [2]. Unlike the pearlitic reaction in Fe–C alloys, where the solution is interstitial in nature, the eutectoid transformation in a substitutional solid solution involves diffusion of the solute atoms either through the matrix or along the boundaries or ledges [3]. For instance, the migrating boundary or reaction front (RF) is known to provide a short-circuit path of diffusion for the eutectoid change in Al–Zn [4]. Recently, the eutectoid change in the Cu–Al system, previously thought to be controlled by volume diffusion [5], has been identified to undergo a ledge-growth mechanism of eutectoid transformation aided by boundary diffusion [6]. Regarding eutectoid decomposition in Cu–In, Spencer and Mack [7] suggested that a compositional adjustment

behind the RF was necessary to produce the equilibrium transformation products. Furthermore, a different type of reaction by which the β phase could assume a herring-bone appearance was observed at temperatures well below T_{eu} such that a pre-precipitation of α preceded a gradual transformation of the matrix (β) to δ. These observations by Spencer and Mack appeared to suggest that the eutectoid transformation in the Cu–In system could be volume-diffusion controlled. However, both Bhatia and Gupta [8] and Manna *et al.* [9] have subsequently carried out kinetic analysis of the isothermal eutectoid growth to conclude that the concerned phase transformation in the Cu–In system is a boundary-diffusion-controlled process. However, both these studies were confined to kinetic analysis based on only a few of the relevant models of eutectoid transformation.

In the present work, an extensive kinetic analysis of the steady-state isothermal eutectoid growth in the Cu–In system has been undertaken considering all the relevant models [4, 10–16] reported in the literature to verify the mode of diffusion during the phase

---

* Author for all correspondence.

transformation. In addition, a detailed differential scanning calorimetric (DSC) analysis has been carried out to substantiate the results of above-mentioned kinetic analysis. It may be pointed out that a similar thermal analysis has earlier been successfully applied to determine the activation energy of discontinuous precipitation [17] and eutectoid transformation [18] in Al–Zn, but has not been utilized for the eutectoid change in the Cu–In system.

2. Experimental procedure

The Cu–20.15 at % In alloy was prepared by induction melting of high purity (>99.99 wt %) copper and indium in an evacuated and argon-filled silica tube. Cylindrical ingots of 10 mm diameter were homogenized at 933 K under similar protective conditions for 14 days and subsequently quenched in iced brine to room temperature. Semicircular discs of 5 mm thickness were cut from the central part of the ingot by a low speed Isomet diamond saw, solution treated at 923 K for 10 h under an argon atmosphere and quenched in iced brine, and subsequently subjected to isothermal ageing by reheating to different predetermined temperatures ($T = 600$ to 825 K), controlled to ± 1 K, in similar evacuated and argon-filled capsules. At a given temperature, the isothermal treatment was interrupted at predetermined intervals of time (t) by quenching in iced brine for microstructural investigation prior to the next treatment with the same sample. A given isothermal treatment was repeated several times to ensure the reproducibility of the results. The isothermally treated samples were ground, polished (with up to 0.1 μm diamond paste) and etched using a colour-tinting solution containing 20 g CrO_3, 2 g Na_2SO_4 and 1.7 ml HCl (35%) in 100 ml distilled water. A detailed microstructural investigation was carried out using a Reichert MEF-2 metallograph and a Jeol scanning electron microscope (SEM) to determine the true eutectoid colony width (w) as a function of t and the true interlamellar spacing (λ) at a given T, respectively. To obtain the true values of w and λ, the average of the maximum growth distances (w_{av}) and interlamellar spacings λ_{av} of a eutectoid colony was calculated from 40–50 random measurements and multiplied by a normalization parameter as in the procedure of Lück [19].

The DSC studies were carried out using small rectangular samples weighing 20–100 mg cut from the homogenized and solution-treated alloy in a Netzsch DTA 404 EP thermal analyser by heating a solution-treated sample at predetermined rates up to 873 K in a sealed aluminium crucible. A given specimen was used only once, but the analysis was repeated several times to ensure the reproducibility of the results. An indigenously developed data acquisition and evaluation software was utilized to analyse the results and evaluate the necessary thermodynamic parameters. For verification, a similar set of samples were subjected to identical thermal treatments in a separate furnace to simulate a typical DSC thermal cycle and correlate the results of such thermal analysis with the corresponding microstructural changes.

3. Results and discussion
3.1. Morphology and distribution of the reaction products

Fig. 1 reveals a typical optical microstructure after eutectoid transformation at 750 K for 2.5 h. The eutectoid colonies (dark) nucleate at the grain boundaries and grow into the untransformed β matrix (light). Here, λ seems too small to be resolved by the optical microscope. Fig. 2a is an SEM micrograph revealing the two-phase lamellar product of the eutectoid transformation at 600 K after 7 h. The parallel alignment and
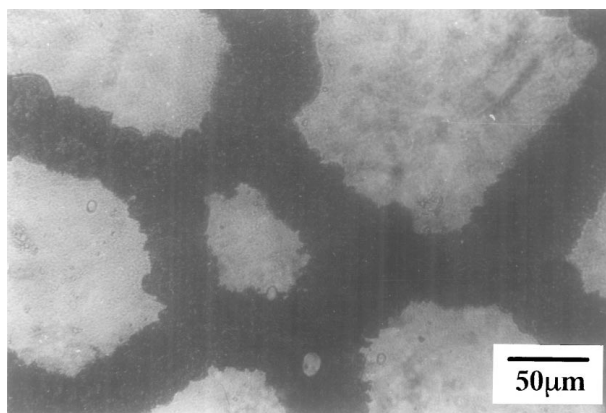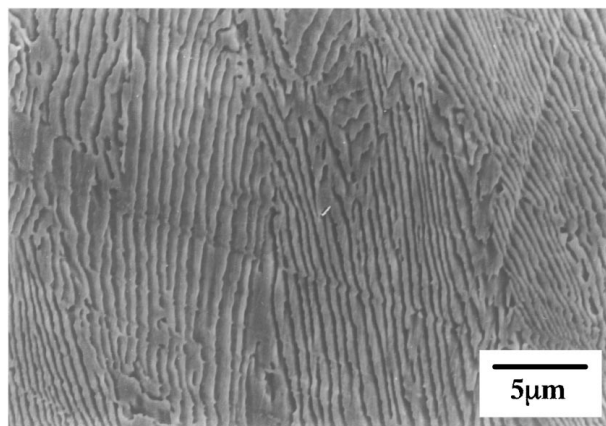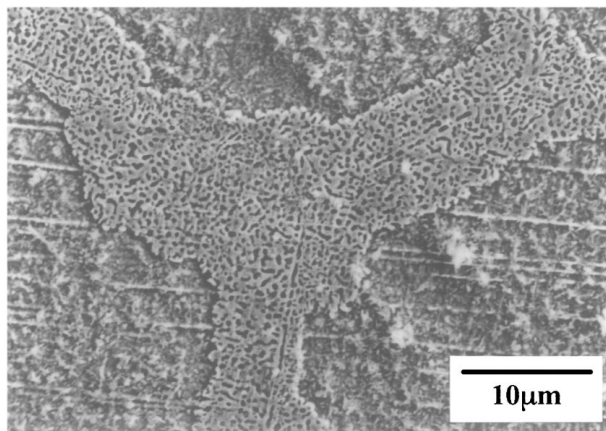

Figure 1 Optical microstructures revealing the eutectoid growth in Cu–20.15 at % In alloy at 750 K after 2.5 h.

(a)

(b)

Figure 2 SEM micrograph of (a) a typical lamellar eutectoid product developed at 600 K after 7 h, and (b) the spherodized morphology of the product phases following eutectoid transformation at 750 K after 1 h.

curved interfaces confirm the lamellar morphology of the transformation product. However, at higher temperatures or extended periods of isothermal treatment, the parallel alignment of the lamellar product tends to be replaced with spherodized or fragmented morphology due to coarsening and/or a low degree of cooperation during the steady-state growth behind the migrating RF (Fig. 2b) [20]. Despite a possible change in the lamellar orientation within a given colony and a tendency to spherodize destroying the parallel orientation between α and δ, it is found that the average repeat distance of δ (center-to-center) is statistically constant at a given temperature.

3.2. Determination of isothermal growth rate

Fig. 3 shows the variation of w as a function of t for different temperatures. It is apparent that w increases with an increase in t at different rates for different isothermal temperatures. The slopes of the w–t plots yield the RF velocity (ν) at a given temperature. It is important to note that the calculation of ν is restricted to the range of a given plot that strictly maintains a linear relationship between w and t (within a standard deviation of 6%). Fig. 4 shows the variation of ν as a function of T. In the temperature range studied, ν increases monotonically with T and does not show a 'C-curve' behavior typical of a diffusion-controlled nucleation and growth process. Significant interference of a concurrent mode of decomposition of β made the distinction of the eutectoid colonies in the microstructure extremely difficult and prevented precise monitoring of the eutectoid colony growth kinetics at $T > 750$ K. It is presumed that a volume-diffusion-controlled mechanism may account for a concurrent mode of decomposition of β along with the usual eutectoid transformation mechanism at
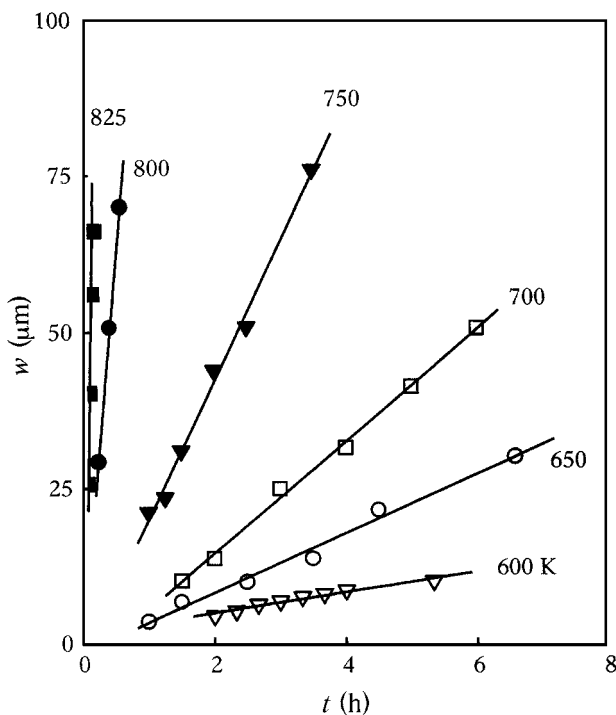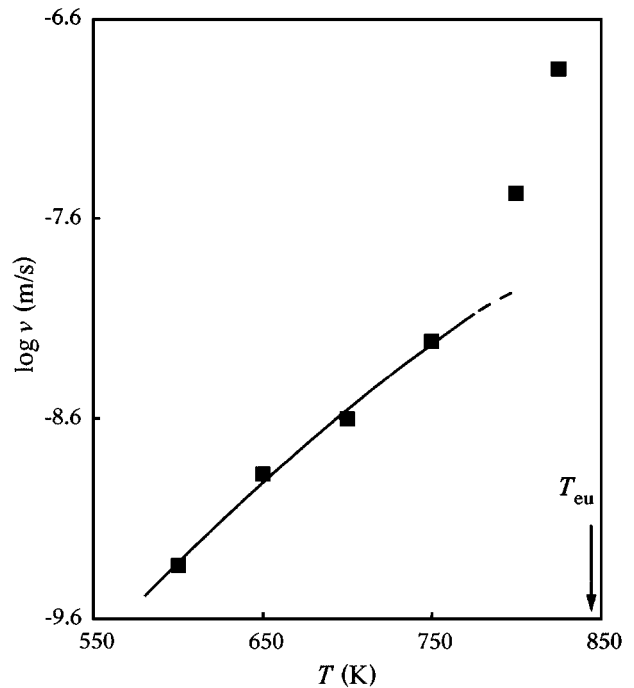

Figure 4 Variation of ν as a function of T.

such elevated temperatures [20]. As a result, w and consequently ν calculated for $T > 750$ K may be grossly overestimated. Hence, the ν–T curve in Fig. 4 is shown as a continuous line only up to 750 K. A possible reversal in the ν–T curve could have been recorded only if the eutectoid colony could be clearly distinguished from the prior β regions in the microstructure following isothermal ageing in the range 750 K $< T < T_{\text{eu}}$.

3.3. Determination of interphase boundary diffusivity

The interphase diffusivity triple product ($s\delta_b D_i$) in terms of the experimentally determined kinetic parameters (ν and λ) may be obtained through kinetic analysis of the eutectoid transformation as [20]

$$s\delta_b D_i = k\lambda^2 \nu \tag{1}$$

where s is the segregation factor, δ_b is the boundary width, D_i is the interface diffusion coefficient, and k is a thermodynamic function related to the concentration terms of the concerned phases.

Turnbull [10] was the first to modify Zener's treatment of the volume-diffusion-controlled eutectoid transformation [11], assuming diffusion to take place through the width of the migrating boundary, and to extend the analysis to discontinuous precipitation. According to Turnbull's approach of growth kinetics, the triple product for the eutectoid transformation may be defined as [12]

$$s\delta_b D_i = \frac{8\nu(x_{\beta/\alpha} - x_{\beta/\delta})}{f_\alpha f_\delta(x_\delta - x_\alpha)} \frac{1}{\lambda^2}\left(1 - \frac{\lambda_c}{\lambda}\right) \tag{2}$$

where $x_{\beta/\alpha}$ and $x_{\beta/\delta}$ are the respective solute concentrations existing in β near the β/α and β/δ interfacial segments, f_α and f_δ are the relative amounts of the two

Figure 3 Variation of w as a function of t at different isothermal T.

product phases, and x_δ and x_α are the equilibrium concentrations of the δ and α phases, respectively. λ_c is the critical spacing for the case where the available driving force (ΔG) for the transformation would be consumed only for the creation of the α/δ interfaces.

Assuming diffusion to take place through a flat boundary of thickness δ_b, Hillert [13] presented an analysis analogous to that for volume-diffusion-controlled growth to derive a final expression of the form

$$s\delta_b D_i = \frac{12\nu\lambda^2(x_{\beta/\alpha} - x_{\beta/\delta})}{\lambda_\alpha\lambda_\delta(x_\delta - x_\alpha)}\frac{1}{\lambda^2}\left(1 - \frac{\lambda_o}{\lambda}\right) \quad (3)$$

where λ_α and λ_δ are the respective spacings of the α and δ phases in the lamellar product. The term λ_o, the spacing for zero growth rate, is defined by the expression

$$2\sigma V_m/\lambda_o =$$
$$(x_{\beta/\alpha} - x_{\beta/\delta})RT f_\alpha f_\delta[(x_\delta - x_\alpha)/(1 - x_\beta)x_\beta] \quad (4)$$

where σ is the specific surface energy of the α/δ interface, V_m is the molar volume, x_β is the original composition of the parent β phase, and R is the gas constant.

Cahn and Hagel [14] also utilized a similar approach to arrive at an expression for the triple product as follows

$$s\delta_b D_i = \frac{2\pi^2\nu(x_{\beta/\alpha} - x_{\beta/\delta})}{x_\delta - x_\alpha}\frac{1}{\lambda^2}. \quad (5)$$

Cheetham and Ridley [4], by modifying the model of Cahn and Hagel, derived an identical expression for the triple product which differs only in the proportionality term used. The final expression is of the form

$$s\delta_b D_i = \frac{4\pi^2\nu(x_{\beta/\alpha} - x_{\beta/\delta})}{x_\delta - x_\alpha}\frac{1}{\lambda^2}. \quad (6)$$

In another treatment, Shapiro and Kirkaldy [15] derived an expression for the boundary-diffusion-controlled growth of the eutectoid by considering local equilibrium across a curved RF providing a short-circuit path of diffusion. In the special case of a symmetrical eutectoid (in terms of the equilibrium compositions of the concerned phases) and parabolic shape of the corresponding free energy curves, the following expression was derived for the triple product

$$s\delta_b D_i = \frac{24\nu}{\lambda^2}\left(\frac{x_{\beta/\alpha} - x_{\beta/\delta}}{0.5 - x_\alpha}\right)\left(1 + \frac{2\sigma V_m}{\Delta G\lambda}\right). \quad (7)$$

Considering $\lambda_c = 2\sigma V_m/\Delta G$, Equation 6 reduces to the more convenient form

$$s\delta_b D_i = \frac{24\nu}{\lambda^2}\left(\frac{x_{\beta/\alpha} - x_{\beta/\delta}}{0.5 - x_\alpha}\right)\left(1 - \frac{\lambda_c}{\lambda}\right). \quad (8)$$

The relationship between λ and λ_c is obtained from the optimization principle based on the maximum growth rate [11, 21] as $\lambda = 1.5\lambda_c$. However, it should be noted that λ_o (as used in Hillert's model, Equation 3), is usu-

ally larger than λ_c because a marginal amount of longitudinal (edgewise) diffusion can never be prevented, even when lateral (sidewise) diffusion is totally precluded. However, the difference between λ_c and λ_o is insignificant in the case of the eutectoid transformation [12]. Similarly, λ_α and λ_δ have been related to λ through a mass balance assuming equal molar volumes for α and δ, so that $\lambda_\alpha = f_\alpha\lambda$ and $\lambda_\delta = f_\delta\lambda$ [20].

Apart from the above-mentioned models used for the calculation of the interphase-diffusivity triple product, the model presented by Sundquist [16] readily accounts for the determination of the activation energy (Q_i) for the operating diffusion process. This model assumes local equilibrium across the interfaces involved and considers the effects of capillary action and non-uniform carbon segregation for the kinetic analysis of boundary-diffusion-controlled eutectoid change. In addition to presenting a numerical solution of the proposed model, an approximate treatment for the general case of the eutectoid transformation by boundary diffusion was also proposed. Accordingly, the temperature dependence of the rate of edgewise growth of pearlite in this analysis may be expressed as

$$\nu \propto (\Delta T)^3 \exp(-Q_i/RT) \quad (9)$$

where Q_i is the activation energy of the process and ΔT is the undercooling at temperatures below T_{eu}.

The experimentally determined values of ν, λ and the concentration-related term $(x_\delta - x_\alpha)/(x_{\beta/\alpha} - x_{\beta/\delta})$ are presented in Table I. The parameters $x_{\beta/\alpha}$ and $x_{\beta/\delta}$ are calculated by suitable extrapolation of the $(\alpha + \beta)/\beta$ and $\beta/(\delta + \beta)$ phase boundaries to the appropriate isothermal transformation temperature. On the other hand, x_α and x_δ are directly obtained from the corresponding equilibrium solvus curves for α and δ, respectively. The $s\delta_b D_i$ values calculated using the relevant kinetic models and experimental data obtained in this study (Table I) at the various isothermal temperatures have been summarized in Table II.

3.4. Determination of the Arrhenius parameters

The temperature dependence of $s\delta_b D_i$ may be expressed in the following form

$$s\delta_b D_i = (s\delta_b D_i)_o \exp(-Q_i/RT) \quad (10)$$

where Q_i is the activation energy for interphase boundary chemical diffusion and $(s\delta_b D_i)_o$ is the pre-exponential factor. Fig. 5 presents the Arrhenius

TABLE I Experimentally determined values of ν, λ and $(x_\delta - x_\alpha)/(x_{\beta/\alpha} - x_{\beta/\delta})$ for different isothermal temperatures

T (K)	ν (m s^{-1})	λ (μm)	$(x_\delta - x_\alpha)/(x_{\beta/\alpha} - x_{\beta/\delta})$
600	4.65×10^{-10}	0.385	2.20
650	1.34×10^{-9}	0.489	2.72
700	2.51×10^{-9}	0.688	3.41
750	6.16×10^{-9}	0.925	4.59
800	3.39×10^{-8}	0.949	7.84
825	1.43×10^{-7}	1.415	16.64

TABLE II $s\delta_b D_i$ values as a function of T calculated for the eutectoid transformation in Cu–20.15 at % In alloy using the different kinetic models available in the literature

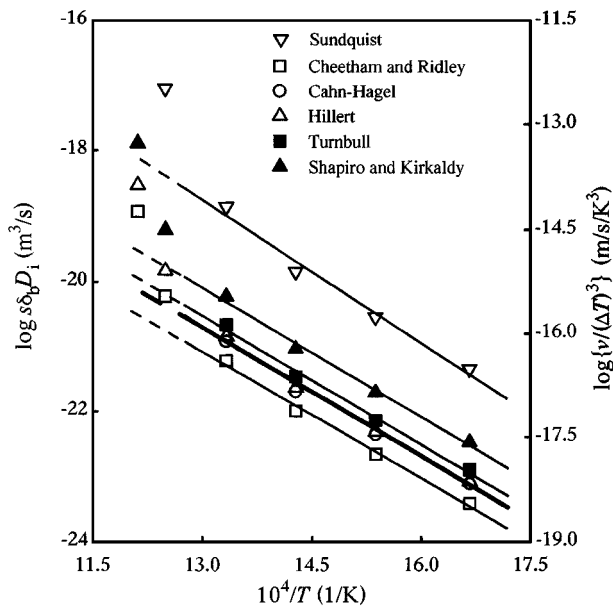|	$s\delta_b D_i(m^3\ s^{-1})$				
T (K)	Cheetham & Ridley	Cahn & Hagel	Hillert	Turnbull	Shapiro & Kirkaldy
600	3.84×10^{-24}	7.68×10^{-24}	8.35×10^{-24}	1.25×10^{-23}	3.36×10^{-23}
650	2.19×10^{-23}	4.39×10^{-23}	4.84×10^{-23}	7.26×10^{-23}	1.94×10^{-22}
700	1.03×10^{-22}	2.05×10^{-22}	2.32×10^{-22}	3.49×10^{-22}	9.33×10^{-22}
750	6.13×10^{-22}	1.23×10^{-21}	1.46×10^{-21}	2.19×10^{-21}	5.94×10^{-21}
800	6.05×10^{-21}	1.21×10^{-20}	1.48×10^{-20}	2.23×10^{-20}	6.25×10^{-20}
825	1.20×10^{-19}	—	2.96×10^{-19}	—	1.27×10^{-18}

Figure 5 Arrhenius plots of $s\delta_b D_i$ obtained from the kinetic analysis of the isothermal growth of the eutectoid transformation using various models.

plots of $s\delta_b D_i$ calculated using Equations 2–6 and 8. In addition, the variation of $\nu/(\Delta T)^3$ as a function of T^{-1} according to Equation 9 is also plotted in Fig. 5 for comparison. Least-square analysis of the respective sets of data in Fig. 5 permits the determination of Q_i and/or $(s\delta_b D_i)_o$ (Table III). Note that the data in Fig. 5 have deviated from linearity at $T > 750$ K due to an overestimation of ν arising out of a possible concurrent mode of decomposition of β [20]. The Q_i values calculated from the present kinetic analysis lie in the range 125–131 kJ mol^{-1} and corresponding $(s\delta_b D_i)_o$ values vary within 2.6×10^{-13} to 3.7×10^{-12} m^3 s^{-1}. Table IV presents a suitable comparison of the results obtained in this study with the relevant data reported in the liter-

TABLE III Arrhenius parameters for interphase-boundary chemical diffusion obtained through kinetic analysis of the eutectoid transformation in Cu–20.15 at % In alloy

Model	Q_i (kJ mol^{-1})	$(s\delta D_i)_o$ (m^3 s^{-1})
Cahn and Hagel	125.0	5.24×10^{-13}
Cheetham and Ridley	125.0	2.62×10^{-13}
Hillert	127.2	8.80×10^{-13}
Turnbull	127.2	1.32×10^{-12}
Shapiro and Kirkaldy	127.4	3.68×10^{-12}
Sundquist	131.4	—

ature [8, 22–24]. The Q_i values calculated in this work are almost equal despite the use of different kinetic models and are comparable with the values for boundary diffusion of In in Cu bicrystals. They compare even better with the values for the grain-boundary chemical diffusion of In in Cu–In alloys obtained from the kinetic analysis of discontinuous precipitation and discontinuous coarsening [24] but are considerably lower (i.e. 0.5 of the lower bound) than those for volume diffusion of In in β Cu–In alloy [25]. Most significantly, the $s\delta_b D_i$ values determined in this study are comparable (to the same order of magnitude) with $s\delta_b D_b$ (D_b = grain-boundary diffusivity) [22, 24] and $s\delta_b D_i$ data [8] reported in the literature at similar temperatures. It is thus concluded that the eutectoid transformation in the present alloy is an interphase boundary-diffusion-controlled process.

3.5. Kinetic analysis by DSC study
On heating the solution-treated and quenched specimen from room temperature at controlled rates, a diffused exothermic peak was observed in the DSC plot (Fig. 6).
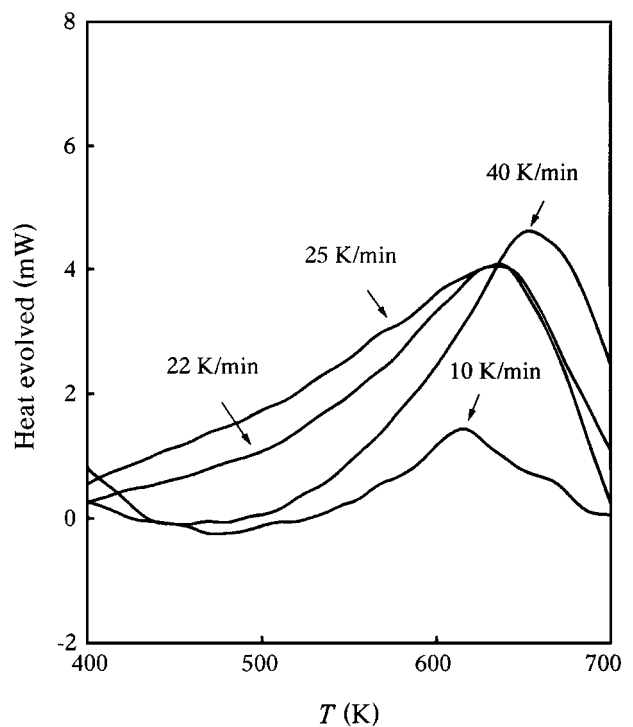
Figure 6 DSC heat flow curves associated with heating the solution-treated and quenched specimens at different heating rates (indicated on each plot).

TABLE IV Comparison of the Arrhenius parameters for In diffusion in Cu–In alloys. DP = discontinuous precipitation, DC = discontinuous coarsening, Q_i = activation energy for interphase-boundary diffusion, Q_b = activation energy for grain-boundary diffusion, Q_v = activation energy for volume diffusion

Type of experiment	Reference	Q_i, Q_b, Q_v (kJ mol^{-1})	$(s\delta D_i)_o$ (m^3 s^{-1})
Eutectoid transformation in Cu–In	This study	125–131	3.7×10^{-12}–2.6×10^{-13}
Boundary diffusion of ^{115}In in Cu	[22]	86	1.2×10^{-14}
DP in Cu–4.6 at % In	[23]	168.3	1.5×10^{-8}
DP in Cu–8.9 at % In	[24]	135–160	
DC in Cu–8.9 at % In	[24]	160 ± 5	
Eutectoid transformation in Cu–In	[8]	130–135	7.2×10^{-12}–4.5×10^{-13}
Volume diffusion of In in β Cu–In	[25]	330 ± 80	$D_o = 5.7 \times 10^{-8}$ m^2 s^{-1}

With an increase in the heating rate, the area under the latter peak increases and the peak itself shifts to a higher temperature. The corresponding microstructure developed on specimens subjected to identical thermal treatment to simulate the DSC cycle has confirmed that the peak in Fig. 6 is associated with the eutectoid transformation of β. Subsequently, the activation energy for the process has been derived from the Ozawa relationship [26] as follows

$$\frac{d \log q}{d(1/T_{max})} = 0.4567\left(\frac{E}{R}\right) \qquad (11)$$

where q is the heating rate, T_{max} is the temperature corresponding to the peak position, and E is the activation energy of the process. Fig. 7 presents the $\log q$ versus $1/T_{max}$ plot for the transformation corresponding to Fig. 6. A suitable regression analysis allows the determination of E from the slope as 133 kJ mol^{-1}. If the specimen is heated beyond the eutectoid temperature (847 K), a sharp endothermic peak is observed, as
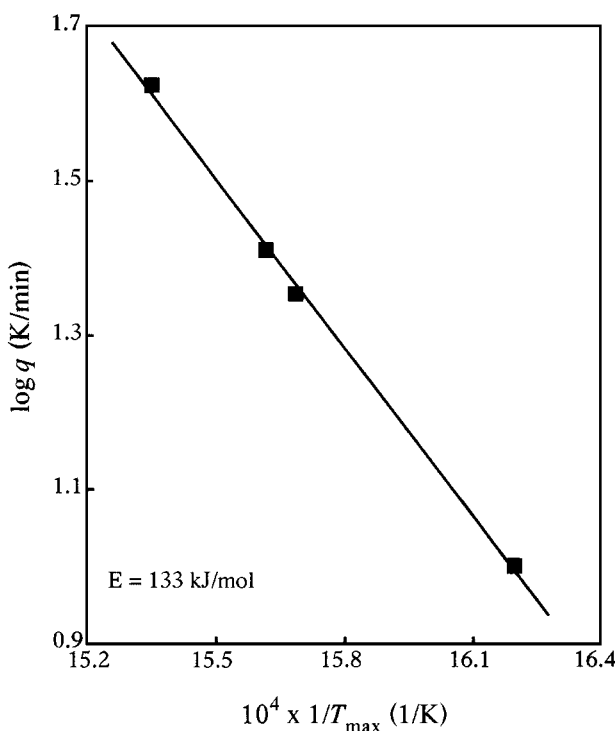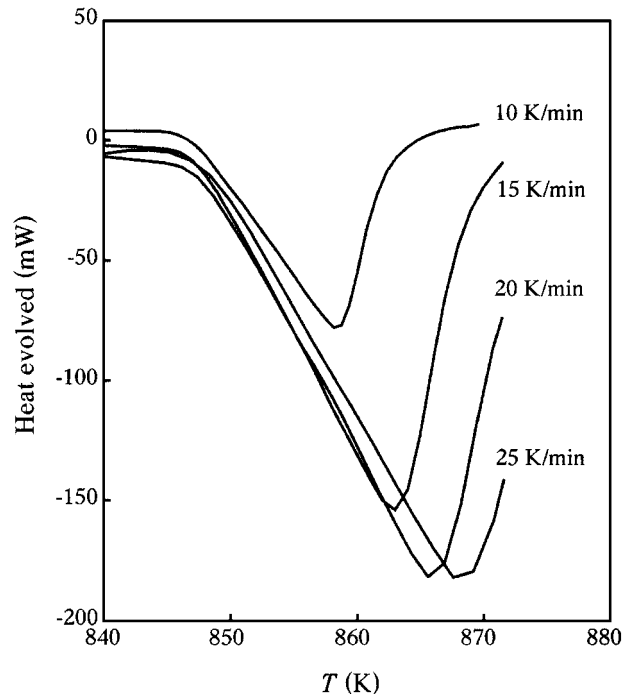

Figure 8 DSC heat flow curves obtained by heating the specimens beyond the eutectoid transformation temperature (847 K) at different heating rates (indicated on each curve).

illustrated in Fig. 8. On increasing the heating rate, the minimum of this endothermic heat effect increases and continuously shifts to a higher temperature (Fig. 8). Fig. 9 presents the Ozawa plot for this endothermic heating effect showing a linear relationship with an activation energy of 591 kJ mol^{-1}. This heating effect occurring beyond the eutectoid isotherm can readily be attributed to the dissolution of the decomposition products of β. The high activation energy of the dissolution process (within the limits of experimental error) may be attributed to a volume-diffusion-controlled transformation. On the other hand, the activation energy of 133 kJ mol^{-1} for the eutectoid transformation is significantly lower than that for the dissolution process. Moreover, it is in good agreement with the activation energy of 125–131 kJ mol^{-1} determined from the isothermal growth kinetics of the eutectoid transformation. Thus, the thermal analysis studies provide further evidence that the eutectoid transformation in the present alloy is an interphase boundary-diffusion-controlled process.
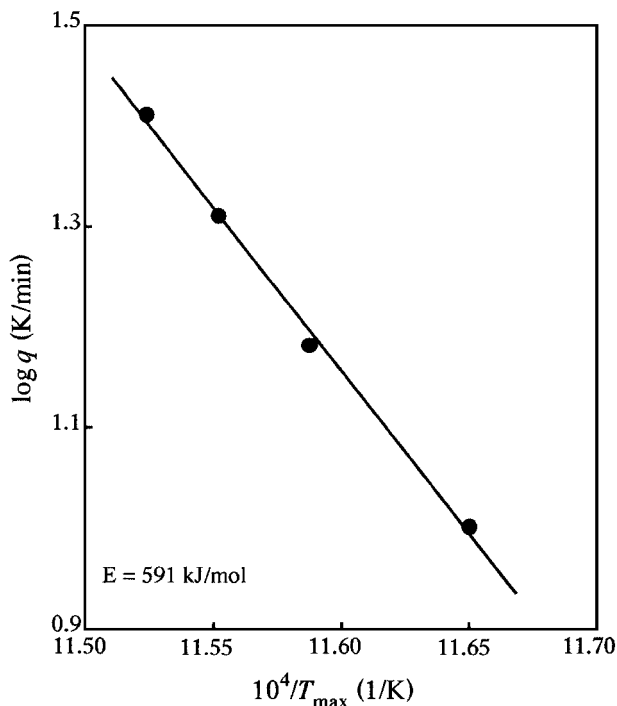

Figure 7 Ozawa plot corresponding to the exothermic peaks in Fig. 6.

Figure 9 Ozawa plot corresponding to the endothermic peaks in Fig. 8.

4. Conclusions

The eutectoid transformation reaction in the Cu–In system initiates at the β/β grain boundaries and the reaction front migrates with a constant velocity during the isothermal growth, maintaining a statistically constant interlamellar spacing in the eutectoid colony behind the growth front. The growth velocity increases with an increase in the isothermal transformation temperature in the temperature range studied. The eutectoid transformation in Cu–20.15 at % In is an interphase boundary-diffusion-controlled process with an activation energy and $(s\,\delta_b D_i)_o$ value lying between 125 and 131 kJ mol^{-1} and between 3.7×10^{-12} and 2.6×10^{-13} m^3 s^{-1}, respectively. Differential scanning calorimetric analysis with the solution-treated and quenched samples reheated at predetermined rates yielded an activation energy of 133 kJ mol^{-1} for the eutectoid transformation of the present alloy (confirmed by subsequent microstructural investigation). The latter is comparable to that calculated from the isothermal-growth kinetic analysis.

Thus, it is concluded that the eutectoid transformation in Cu–In is a boundary-diffusion-controlled process.

References

1. A. D. PELTON, in "Thermodynamics and phase diagrams in materials, materials science and technology," Vol. 5, edited by R. W. Cahn, P. Haasen and E. J. Kramer (VCH Verlagsgesellschaft GmbH, Weinheim, 1991) p. 33.
2. "Binary Alloy Phase Diagrams," Vol. 2, edited by T. B. Massalski (ASM International, Materials Park, Ohio, 1990) p. 1425.
3. M. J. WHITING and P. TSAKIROPOULOS, *Scr. Metall. Mater.* **30** (1994) 1031.
4. D. CHEETHAM and N. RIDLEY, *J. Inst. Met.* **99** (1971) 371.
5. M. P. ASUNDI and D. R. F. WEST, *ibid.* **94** (1966) 327.
6. M. J. WHITING and P. TSAKIROPOULOS, *Mater. Sci. Technol.* **11** (1995) 977.
7. C. W. SPENCER and D. J. MACK, *J. Inst. Met.* **82** (1953–54) 81.
8. M. K. BHATIA and S. P. GUPTA, *Z. Metallkde.* **85** (1994) 192.
9. I. MANNA, A. DAS, S. K. PABI and W. GUST, *Defect Diff. Forum* **143**–**147** (1996) 1551.
10. D. TURNBULL, *Acta Metall.* **3** (1955) 55.
11. C. ZENER, *AIME Trans.* **167** (1946) 550.
12. M. HILLERT, *Metall. Trans.* **3** (1972) 2729.
13. M. HILLERT, in "The mechanism of phase transformations in crystalline solids" (Institute of Metals, London, 1969) p. 231.
14. J. W. CAHN and W. C. HAGEL, in "Decomposition of austenite by diffusional processes," edited by V. F. Zackay and H. I. Aaronson (Interscience Publ., Easton, PA, 1962) p. 131.
15. J. M. SHAPIRO and J. S. KIRKALDY, *Acta Metall.* **16** (1968) 579.
16. B. E. SUNDQUIST, *ibid.* **16** (1968) 1413.
17. W. LACOM, C. Y. ZAHRA and A. M. ZAHRA, *Scr. Metall. Metall.* **23** (1989) 2001.
18. M. VIJAYALAKSHMI, V. SEETHARAMAN and V. S. RANGHUNATHAN, *ibid.* **15** (1981) 985.
19. R. LÜCK, *Z. Metallkde.* **66** (1975) 488.
20. A. DAS, PhD thesis, Indian Institute of Technology, Kharagpur (1997).
21. M. HILLERT, *Jernkontorets Ann.* **141** (1957) 757 (cited in [12]).
22. W. GUST, M. B. HINTZ, A. LODDING, R. LUCIC, H. ODELIUS and U. ROLL, *Mikrochim. Acta, Suppl.* **9** (1981) 307.
23. W. GUST, B. PREDEL and U. ROLL, *Acta Metall.* **28** (1980) 1395.
24. S. P. GUPTA, *ibid.* **34** (1986) 1279.
25. B. G. MELLOR and G. A. CHADWICK, *Met. Sci.* **8** (1974) 63.
26. T. OZAWA, *J. Therm. Anal.* **2** (1970) 301.